Virologica Sinica 39 (2024) 516–519

Contents lists available at ScienceDirect

Virologica Sinica

journal homepage: www.keaipublishing.com/en/journals/virologica-sinica
www.virosin.org

Letter

A lethal mice model of recombinant vesicular stomatitis viruses for EBOV-targeting prophylactic vaccines evaluation

Hong-Qing Zhang [a,b], Zhe-Rui Zhang [a], Cheng-Lin Deng [a], Zhi-Ming Yuan [a,b,c], Bo Zhang [a,b,c,*]

[a] Key Laboratory of Special Pathogens and Biosafety, Wuhan Institute of Virology, Center for Biosafety Mega-Science, Chinese Academy of Sciences, Wuhan, 430071, China
[b] University of Chinese Academy of Sciences, Beijing, 100049, China
[c] Hubei Jiangxia Laboratory, Wuhan, 430200, China

Dear editor,

Ebola virus (EBOV) is a member of the genus *Orthoebolavirus* within the family of *Filoviridae*. It's the causative agent of Ebola virus disease (EVD), characterized by general malaise, severe gastrointestinal illness, febrile, coagulopathy, multi-organs dysfunction, and high mortality (up to 90%) in humans and nonhuman primates (NHPs) (Jacob et al., 2020). Since its discovery in 1976, EBOV has grabbed the global concerns, especially after the West African epidemic from 2014 to 2016, which resulted in 30,000 cases and over 11,000 deaths (Feldmann et al., 2020; Jacob et al., 2020). From 2018 to 2022, there have been thousands of infections primarily in the Democratic Republic of the Congo (DRC), resulting in over 2000 deaths. This highlights the importance of continued attention and ongoing surveillance (www.who.int/emergencies/disease-outbreak-news).

Animal models are essential tools for screening therapeutics and prophylactic vaccines, and various animal models have been developed (Bente et al., 2009; Geisbert et al., 2015), such as nonhuman primates (NHPs) infected with wild type EBOV and rodents with rodent-adapted EBOV. These models can mimic the pathogenicity of EBOV in humans to the greatest extent and are commonly used in vaccines/therapeutics research (Pushko et al., 2000; Geisbert et al., 2015). However, they require high bio-containment biosafety level 4 (BSL-4) facilities and strict manipulation procedures to prevent the contamination of operators and environments. In addition, conducting preclinical studies in BSL-4 facilities also increases the cost and complexity of vaccines and therapeutics evaluation. Therefore, it is important to establish surrogate animal models for *in vivo* antiviral research in standard BSL-2 facilities.

Glycoprotein (GP) is the primary target of neutralizing antibodies against EBOV, responsible for viral attachment and entry (Pallesen et al., 2016). Therefore, designing vaccines and antiviral drugs targeting EBOV GP is the main strategy against EBOV. Recombinant viruses embedded with EBOV GP are the basis for implementing surrogate animal models in standard BSL-2 laboratories. In recent years, the live attenuated EBOV vaccine, replication-competent vesicular stomatitis virus encoding EBOV GP (VSV-EBOV) has been approved by EU and USA with a good safety profile and extensively studied in standard BSL-2 facilities (Garbutt et al., 2004; Lee et al., 2021; Lee et al., 2023). Its embedded EBOV GP, in place of its parental VSV G, confers infectivity to this recombinant virus and could elicit GP-specific antibody with neutralizing activities against EBOV (Garbutt et al., 2004). Therefore, VSV-EBOV can be selected as an alternative to EBOV to eliminate the need for BSL-4 facilities for the researches on GP-associated viral pathogenicity and GP-targeting vaccines in BSL-2 facilities. Surrogate animal models based on VSV-EBOV have been well studied, including neonatal C57BL/6 mice, Syrian hamsters and immunodeficient mice (McWilliams et al., 2019; Saito et al., 2020; Lee et al., 2021). In particular, acute and fatal diseases could be induced in immunodeficient mice after VSV-EBOV infection, such as transcription factor STAT1-knockout ($STAT1^{-/-}$) and interferon α/β receptors-knockout ($IFNAR^{-/-}$) mice (Marzi et al., 2015). This suggests that this model can be used in BSL-2 facilities for evaluation of vaccines by using replication-competent VSV-EBOV instead of wild-type EBOV.

In this study, we found a surrogate EBOV lethal mouse model that can be used in standard BSL-2 facilities by employing type I and II Interferon receptors-knockout ($IFN\alpha/\beta/\gamma\ R^{-/-}$) mice infected with VSV-EBOV. Additionally, Venezuelan equine encephalitis virus (VEEV) replicon particle expressing EBOV GP (EBOV VRP), a previously reported EBOV vaccine candidate (Pushko et al., 2000), showed protective efficacy in this model, suggesting the potential of using this model as a platform for EBOV GP-targeting vaccines evaluation in BSL-2 facilities.

To determine the susceptibility of immunodeficient mice to rVSVΔG-EBOV/GP (designated as VSV-EBOV), cohorts of 129S6/SvEv $IFN\alpha/\beta/\gamma\ R^{-/-}$ mice aged 8–10 weeks were intraperitoneally (i.p.)

* Corresponding author.
E-mail address: zhangbo@wh.iov.cn (B. Zhang).

https://doi.org/10.1016/j.virs.2024.03.008
Received 9 October 2023; Accepted 18 March 2024
Available online 24 March 2024

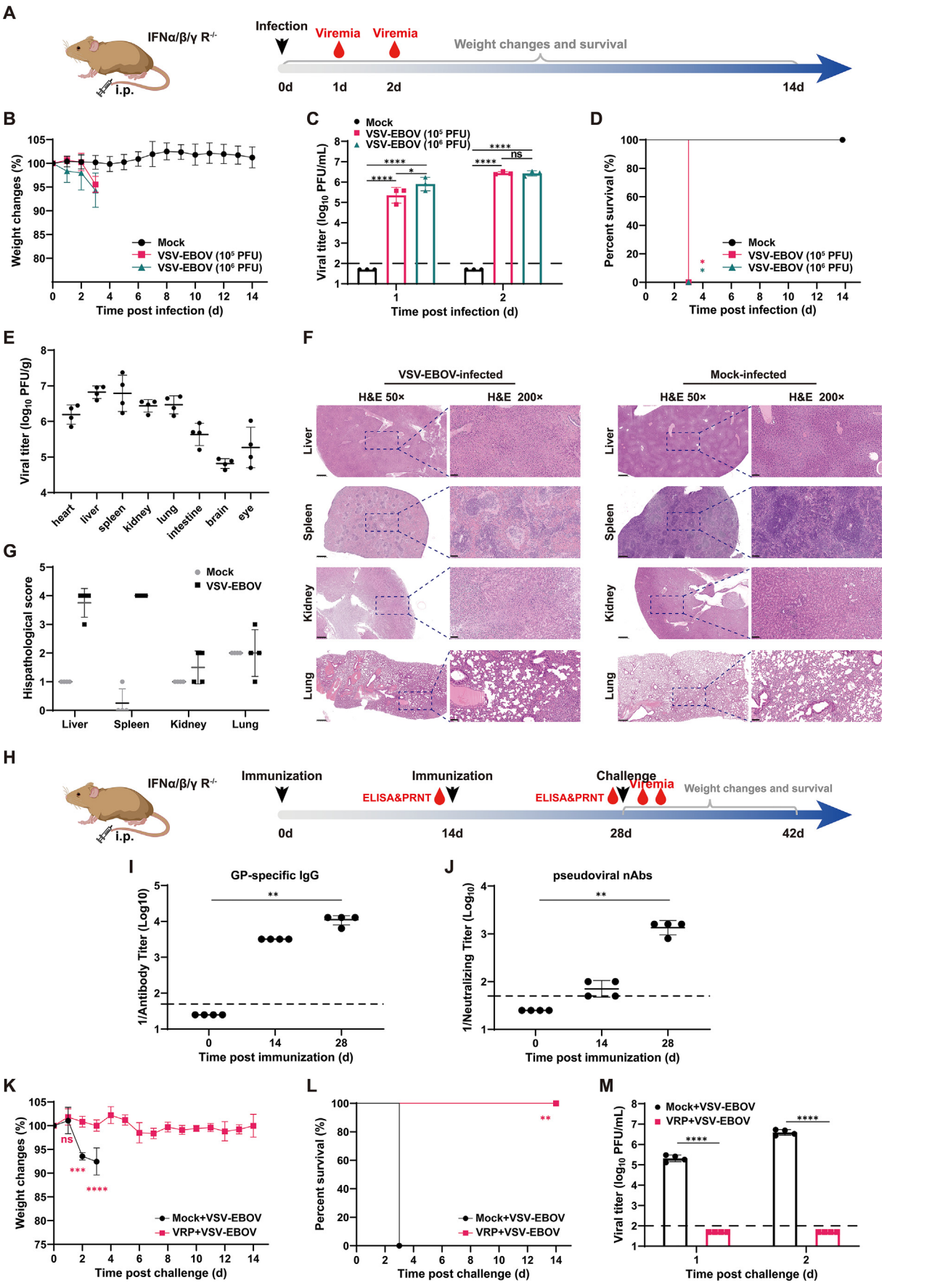

(caption on next page)

Fig. 1. Evaluation of VSV-EBOV infected-IFNα/β/γ $R^{-/-}$ mice as a surrogate EBOV lethal model for vaccine development. **A** Schematic diagram of VSV-EBOV infection in IFNα/β/γ $R^{-/-}$ mice. Cohorts of adult IFNα/β/γ $R^{-/-}$ mice (n = 3) aged 8–10 weeks were intraperitoneally inoculated with 1×10^5 and 1×10^6 PFU VSV-EBOV. Weight changes (**B**) and survival rates (**D**) were recorded daily for 14 days after infection. Viremia (**C**) was detected within the first two days after infection. The blood samples were collected from the orbital of mice. The horizontal dotted line represents the limit of detection: 100 PFU/mL. **E** Tissue tropism and organ virus load of VSV-EBOV in IFNα/β/γ $R^{-/-}$ mice. Mice were i. p. infected with 1×10^6 PFU VSV-EBOV and sacrificed at 2 dpi for tissues collection. Viral loads in different tissues of infected mice were detected at 2 dpi. Liver, spleen, kidney and lung were collected and fixed for hematoxylin and eosin (H&E) staining (**F**) and quantitative pathological scoring (**G**). Scale bars in magnification of 50 × represent 500 μm, in magnification of 200 × represent 100 μm. **H** Schematic diagram of EBOV VRPs vaccination and VSV-EBOV challenge in mice. Group of IFNα/β/γ $R^{-/-}$ mice (n = 4) aged 8–10 weeks were i. p. immunized with 5×10^6 IU EBOV VRPs on day 0 and 14. **I, J** EBOV GP-specific IgG and pVNA were measured by ELISA and plaque reduction neutralization test (PRNT) on day 14 after each immunization. The blood samples were collected from the orbital of mice. The horizontal dotted line represents the limit of detection: 1:50. On day 28, the immunized mice were i. p. challenged with 1×10^5 PFU VSV-EBOV. Clinical symptoms, weight changes (**K**) and survival rates (**L**) were monitored daily for 14 days. **M** The viremia was detected within the first two days after challenge. The horizontal dotted line represents the limit of detection: 100 PFU/mL. Data represent the geometrical mean ± standard deviation at each time point in each group. The asterisks denote statistical differences between the indicated groups. n. s., no statistical difference, *, $P < 0.05$; **, $P < 0.01$; ***, $P < 0.001$; ****, $P < 0.0001$.

inoculated with two doses of VSV-EBOV (1×10^5 and 1×10^6 PFU) and monitored for clinical symptoms and weight changes daily during 14 days after infection (Fig. 1A). All infected IFNα/β/γ $R^{-/-}$ mice exhibited a significant decrease in vitality and 5%–10% weight loss after infection (Fig. 1B), and finally succumbed (Fig. 1D) at 3 days post infection (dpi). Besides, high levels of viremia could be detected in IFNα/β/γ $R^{-/-}$ mice, reaching 10^5–10^6 PFU/mL at 1 dpi and increasing to 10^6–10^7 PFU/mL at 2 dpi (Fig. 1C). To further characterize the pathogenicity of VSV-EBOV, IFNα/β/γ $R^{-/-}$ mice were inoculated with serially diluted VSV-EBOVs (ranged from 1×10^2 to 1×10^5 PFU) via i.p. route (Supplementary Fig. S1A). We found that the infected mice developed a dose-dependent viremia at 1 dpi, and the viral load rapidly increased to similar levels of approximately 10^6–10^7 PFU/mL (Supplementary Fig. S1C). In addition, all mice succumbed at 3 dpi except one mouse in the lowest infection dose of 1×10^2 PFU with one day delay (Supplementary Figs. S1C and S1D), exhibiting approximate 5%–10% weight loss (Supplementary Fig. S1B). These data indicated that IFNα/β/γ $R^{-/-}$ mice were highly susceptible to VSV-EBOV with severe diseases and lethal phenotype.

Further analysis was conducted to determine the tissue tropism and organ virus load. IFNα/β/γ $R^{-/-}$ mice were infected with 1×10^6 PFU VSV-EBOV and euthanized at 2 dpi for tissue collection, including heart, liver, spleen, lung, kidney, intestine, brain and eye (Fig. 1E). As expected, VSV-EBOV could be detected in all the tissues, with the key target being liver, spleen, kidney and lung (Fig. 1E). Having established that VSV-EBOV infects various tissues of IFNα/β/γ $R^{-/-}$ mice, we next assessed whether the infection was associated with pathologic changes. On day 2 after VSV-EBOV infection, IFNα/β/γ $R^{-/-}$ mice were sacrificed for tissues collection, including liver, spleen, kidney and lung. The hematoxylin-eosin (H&E) staining results showed that evident histologic lesions were observed in livers (unclear hepatic lobular structure, hepatocyte hemorrhage and necrosis, a little steatosis, and scattered chronic inflammatory cell infiltration) and spleens (atrophy of splenic bodies, congestion of red pulp, marked reduction and partial necrosis of lymphocytes) of all the VSV-EBOV infected mice (Fig. 1F), which was similar to the histopathological features of authentic EBOV infection in rodents (Raymond et al., 2011; Cross et al., 2015). In contrast, there were no significant differences in another two organs between the two groups (Fig. 1F), only mild spontaneous lesions in the kidney (slight atrophy of the small renal tubules and occlusion of the glomerular capillary network) and lung (slight thickening of the alveolar septum and congestion of the blood vessels). In addition, quantitative pathological scoring showed the same trends with the H&E observation (Fig. 1G). Taken together, VSV-EBOV infection caused severe liver and spleen lesions in IFNα/β/γ $R^{-/-}$ mice.

Viral replicon particles (VRPs) are single infectious viral particles generated by *trans*-complementation with VEEV structural proteins, serving as a vehicle for delivering self-replicating RNA that efficiently expresses exogenous proteins (Pushko et al., 2000). *In vivo* administration of EBOV VRPs expressing EBOV GP was reported to provide potent protection in both rodents and NHPs models against wild-type EBOV lethal challenge (Pushko et al., 2000; Herbert et al., 2013). We constructed the VEEV replicon bearing EBOV-GP (VEEV-EBOVGP) and EBOV VRPs as described in Supplementary Materials. GP-specific immunofluorescence signals (Supplementary Figs. S2A and S2B) and chemiluminescence bands (~130 kDa) (Supplementary Figs. S2C and S2D) were detected in both VEEV-EBOVGP transfected- and EBOV VRPs infected-cells, suggesting that the self-replicating VEEV-EBOVGP replicon can be efficiently delivered by EBOV VRPs.

On this basis, we utilized the EBOV VRPs to evaluate whether IFNα/β/γ $R^{-/-}$ mice can be used as a platform for *in vivo* evaluation of prophylactic vaccines against EBOV. Group of IFNα/β/γ $R^{-/-}$ mice aged 8–10 weeks were i. p. immunized with two doses of 5×10^6 IU EBOV VRPs with two weeks intervals (Fig. 1H). On day 14 after first immunization, considerable EBOV GP-specific IgG antibodies and pseudoviral neutralizing antibodies (pVNA) were detected with geometrical mean titers (GMT) of 1/3200 and 1/71, respectively (Fig. 1I and J). Booster vaccination induced a further increase in IgG and pVNA with GMT of 1/10,763 and 1/1345 on day 28 (Fig. 1I and J). Then all mice were challenged with 1×10^5 PFU VSV-EBOV via i. p. route, and monitored daily for clinical symptoms and weight changes (Fig. 1H). VRPs-treated mice were fully protected to survive, exhibiting no signs of illness or weight loss (Fig. 1K–L). Undetectable viremia during the first two days after challenge also supported the superior efficacy for EBOV VRPs (Fig. 1M). In contrast, all PBS-treated mice developed disease rapidly and succumbed at 3 dpi with high levels of viremia (Fig. 1K–M). Collectively, these data demonstrated that VSV-EBOV-infected IFNα/β/γ $R^{-/-}$ mice could be used as an effective animal model for vaccine evaluation against EBOV in BSL-2 facilities.

In summary, we observed acute and fatal outcomes in IFNα/β/γ $R^{-/-}$ mice after VSV-EBOV infection, including hyperviremia, weight loss and hispathology of the liver and spleen. Moreover, EBOV VRPs, a reported vaccine candidate against EBOV (Pushko et al., 2000), were also shown to be effective in VSV-EBOV-infected IFNα/β/γ $R^{-/-}$ mice. Due to the expression of EBOV GP and the limited biological risk of VSV-EBOV, this surrogate animal model could serve as a useful tool for *in vivo* screening of therapeutics and vaccines against EBOV targeting GP in BSL-2 facilities, rather than BSL-4 ones.

Footnotes

This work was supported by the National Natural Science Foundation of China (Grant No. U20A2014) and the Strategic Priority Research Program of the Chinese Academy of Sciences (Grant No. XDB0490000). The funders had no role in study design, data collection and interpretation, or the decision to submit the work for publication. We are grateful to the Center for Animal Experiments staff (Xue-fang An, Fan Zhang, He Zhao, Li Li, Tao Zhang and Yuzhou Xiao) at the Wuhan Institute of Virology and the Wuhan Key Laboratory of Special Pathogens and Biosafety for helpful support during the course of the work. The authors declare that they have no conflict of interest. Prof. Bo Zhang is an editorial board member for *Virologica Sinica* and was not involved in the

editorial review or the decision to publish this article. All the mice were cared following the recommendations of National Institutes of Health Guidelines for the Care and Use of Experimental Animals. Studies related to virus infection were performed in biosafety level 2 (BSL-2) facility at Wuhan Institute of Virology under a protocol approved by the Laboratory Animal Ethics Committee of Wuhan Institute of Virology, Chinese Academy of Sciences (WIVA26202301).

Supplementary data to this article can be found online at https://doi.org/10.1016/j.virs.2024.03.008.

References

Bente, D., Gren, J., Strong, J.E., Feldmann, H., 2009. Disease modeling for ebola and marburg viruses. Dis Model Mech 2, 12–17.

Cross, R.W., Fenton, K.A., Geisbert, J.B., Mire, C.E., Geisbert, T.W., 2015. Modeling the disease course of zaire ebolavirus infection in the outbred Guinea pig. J. Infect. Dis. 212 (Suppl. 2), S305–S315.

Feldmann, H., Sprecher, A., Geisbert, T.W., 2020. Ebola. N. Engl. J. Med. 382, 1832–1842.

Garbutt, M., Liebscher, R., Wahl-Jensen, V., Jones, S., Moller, P., Wagner, R., Volchkov, V., Klenk, H.D., Feldmann, H., Stroher, U., 2004. Properties of replication-competent vesicular stomatitis virus vectors expressing glycoproteins of filoviruses and arenaviruses. J. Virol. 78, 5458–5465.

Geisbert, T.W., Strong, J.E., Feldmann, H., 2015. Considerations in the use of nonhuman primate models of ebola virus and marburg virus infection. J. Infect. Dis. 212 (Suppl. 2), S91–S97.

Herbert, A.S., Kuehne, A.I., Barth, J.F., Ortiz, R.A., Nichols, D.K., Zak, S.E., Stonier, S.W., Muhammad, M.A., Bakken, R.R., Prugar, L.I., Olinger, G.G., Groebner, J.L., Lee, J.S., Pratt, W.D., Custer, M., Kamrud, K.I., Smith, J.F., Hart, M.K., Dye, J.M., 2013. Venezuelan equine encephalitis virus replicon particle vaccine protects nonhuman primates from intramuscular and aerosol challenge with ebolavirus. J. Virol. 87, 4952–4964.

Jacob, S.T., Crozier, I., Fischer 2nd, W.A., Hewlett, A., Kraft, C.S., Vega, M.A., Soka, M.J., Wahl, V., Griffiths, A., Bollinger, L., Kuhn, J.H., 2020. Ebola virus disease. Nat. Rev. Dis. Prim. 6, 13.

Lee, A.W., Liu, K., Lhomme, E., Blie, J., McCullough, J., Onorato, M.T., Connor, L., Simon, J., Dubey, S., VanRheenen, S., Deutsch, J., Owens, A., Morgan, A., Welebob, C., Hyatt, D., Nair, S., Hamze, B., Guindo, O., Sow, S.O., Beavogui, A.H., Leigh, B., Samai, M., Akoo, P., Serry-Bangura, A., Fleck, S., Secka, F., Lowe, B., Watson-Jones, D., Roy, C., Hensley, L.E., Kieh, M., Coller, B.G., Team, P.S., 2023. Immunogenicity and vaccine shedding after 1 or 2 doses of rvzvdeltag-zebov-gp ebola vaccine (ervebo(r)): results from a phase 2, randomized, placebo-controlled trial in children and adults. Clin. Infect. Dis. https://doi.org/10.1093/cid/ciad693.

Lee, H.N., McWilliams, I.L., Lewkowicz, A.P., Engel, K., Ireland, D.D.C., Kelley-Baker, L., Thacker, S., Piccardo, P., Manangeeswaran, M., Verthelyi, D., 2021. Characterization of the therapeutic effect of antibodies targeting the ebola glycoprotein using a novel bsl2-compliant rvsvdeltag-ebov-gp infection model. Emerg. Microb. Infect. 10, 2076–2089.

Marzi, A., Kercher, L., Marceau, J., York, A., Callsion, J., Gardner, D.J., Geisbert, T.W., Feldmann, H., 2015. Stat1-deficient mice are not an appropriate model for efficacy testing of recombinant vesicular stomatitis virus-based filovirus vaccines. J. Infect. Dis. 212 (Suppl. 2), S404–S409.

McWilliams, I.L., Kielczewski, J.L., Ireland, D.D.C., Sykes, J.S., Lewkowicz, A.P., Konduru, K., Xu, B.C., Chan, C.C., Caspi, R.R., Manangeeswaran, M., Verthelyi, D., 2019. Pseudovirus rvsvdeltag-zebov-gp infects neurons in retina and cns, causing apoptosis and neurodegeneration in neonatal mice. Cell Rep. 26, 1718–1726 e1714.

Pallesen, J., Murin, C.D., de Val, N., Cottrell, C.A., Hastie, K.M., Turner, H.L., Fusco, M.L., Flyak, A.I., Zeitlin, L., Crowe Jr., J.E., Andersen, K.G., Saphire, E.O., Ward, A.B., 2016. Structures of ebola virus gp and sgp in complex with therapeutic antibodies. Nat Microbiol 1, 16128.

Pushko, P., Bray, M., Ludwig, G.V., Parker, M., Schmaljohn, A., Sanchez, A., Jahrling, P.B., Smith, J.F., 2000. Recombinant rna replicons derived from attenuated venezuelan equine encephalitis virus protect Guinea pigs and mice from ebola hemorrhagic fever virus. Vaccine 19, 142–153.

Raymond, J., Bradfute, S., Bray, M., 2011. Filovirus infection of stat-1 knockout mice. J. Infect. Dis. 204 (Suppl. 3), S986–S990.

Saito, T., Maruyama, J., Nagata, N., Isono, M., Okuya, K., Takadate, Y., Kida, Y., Miyamoto, H., Mori-Kajihara, A., Hattori, T., Furuyama, W., Ogawa, S., Iida, S., Takada, A., 2020. A surrogate animal model for screening of ebola and marburg glycoprotein-targeting drugs using pseudotyped vesicular stomatitis viruses. Viruses 12, 923.